Heterogeneous Catalysis in the Liquid-phase Oxidation of Olefins. IV. The Activity of a Supported Vanadium or Chromium Oxide Catalyst in the Decomposition of *t*-Butyl Hydroperoxide

Katsuomi TAKEHIRA,* Takashi HAYAKAWA, and Toshio ISHIKAWA

Catalysis Division, National Chemical Laboratory for Industry, Tsukuba Research Center, Yatabe, Ibaraki 305

(Received March 17, 1979)

The liquid-phase decomposition of *t*-butyl hydroperoxide (*t*-BuOOH) has been carried out in benzene under an N_2 atmosphere using a vanadium or chromium oxide, supported on γ-Al_2O_3 or SiO_2 as the catalyst, for the purpose of clarifying the reaction mechanism of the cyclohexene oxidation. The decomposition of *t*-BuOOH on the supported oxide catalyst was a first-order reaction; the main products were *t*-butyl alcohol, di-*t*-butyl peroxide, and acetone, suggesting that *t*-BuOOH is decomposed homolytically on the catalyst by the Haber-Weiss mechanism. The effect of the vanadium–chromium binary system formation was small, but the interaction between metal oxides and the supports appeared to be important in the *t*-BuOOH decomposition. Tetrahedrally co-ordinated vanadium species were formed on SiO_2 and showed the highest activity, followed by the chromium co-ordinated tetrahedrally on SiO_2 or on γ-Al_2O_3, while an octahedrally co-ordinated vanadium or chromium showed low activity. Such order of the activity was in good agreement with that obtained in the liquid-phase oxidation of cyclohexene. We observed a relatively good correlation between the catalytic activity and the acidity of the supported binary metal oxides. The V_2O_5–SiO_2 system showed an especially large acidity; here *t*-butyl alcohol was dehydrated into di-*t*-butyl ether and 2-methyl propene.

The liquid-phase oxidation of cyclohexene with a heterogeneous catalyst, *i.e.*, vanadium–chromium binary oxides (V–Cr), has been studied in terms of the relationship between its structure and the catalytic activity.[1-3] When the binary system was supported on γ-Al_2O_3 or SiO_2, its activity varied greatly depending on the nature of the carrier.[1] It was suggested that the activity of the supported binary system is mainly due to the interactions between the metal oxides and the carrier; a tetrahedral co-ordination is favored on SiO_2, resulting in the increase in its activity. It was also suspected that the supported binary system catalyzes the autoxidation of cyclohexene by accelerating the decomposition of 1-cyclohexenyl hydroperoxide.[1] To confirm the validity of this mechanism, the decomposition of *t*-butyl hydroperoxide (*t*-BuOOH) on a supported binary oxide catalyst has been studied in the present work. *t*-BuOOH has been frequently used as a model compound in studying the mechanism of the catalytic decomposition of hydroperoxides because complicating reactions, such as hydration and rearrangement, can be minimized with tertially alkyl hydroperoxide.[4-12] Also, a direct comparison can be made with the other investigations where *t*-BuOOH was used.[4-12] A further study of the structure of the supported binary system has concurrently been carried out by measuring the electron-spin resonance and the surface acidity so as to clarify their roles in the oxidation of cyclohexene.

Experimental

Catalysts. The metal acetylacetonates ($Me(acac)_n$) were used as received (Tokyo Chemical Industry Co.). The supported binary system catalysts were prepared by the kneading method reported in a preceding paper.[1] The symbols, concentrations (calculated as $V_2O_5+Cr_2O_3$(wt %)) and compositions (in terms of atomic % of Cr/(V+Cr)) of the supported metal oxides, and the specific surface area (S_s), are shown in Tables 1 and 2 respectively.

Procedure of Reaction. The decomposition of *t*-BuOOH was performed in 10-ml reaction tubes with a joint which fitted into a smoothtapered joint provided with a stopcock. The same amount of catalyst (25 mg of the binary catalyst or 5×10^{-6} mol of $Me(acac)_n$) was added to a series of reaction tubes, in each of which the reaction was allowed to proceed for a different time interval. A reactor tube containing the weighed catalyst was placed in an ethanol-solid carbon dioxide mixture, and a 5-ml portion of a previously prepared benzene solution of *t*-BuOOH (0.1 M) was slowly added to the reactor to avoid the suspension of the catalyst. The reactor was then joined to a vacuum system, and the gas phase was replaced with dry nitrogen. The stopcock was then closed to isolate the system. The reactor was attached to a wrist-action shaker to achieve vigorous agitation and then plunged into an oil bath, the temperature of which could be controlled to within ±0.2 °C. The time was recorded from the moment the tube was immersed in the oil bath. Once the desired reaction-time interval had elapsed, the tube was quickly put back into the

TABLE 1. CONCENTRATIONS OF SUPPORTED METAL OXIDES, SYMBOLS, AND SPECIFIC SURFACE AREAS OF CATALYSTS

Concentration $V_2O_5+Cr_2O_3$ (wt %)	γ-Al_2O_3-series[a]		SiO_2-series[b]	
	Symbol	S_s(m^2/g)	Symbol	S_s(m^2/g)
0	γ-Al_2O_3	220	SiO_2	210
1	V–Cr–γ-Al_2O_3-(1)	246	V–Cr–SiO_2-(1)	202
5	V–Cr–γ-Al_2O_3-(5)	277	V–Cr–SiO_2-(5)	181
10	V–Cr–γ-Al_2O_3-(10)	293	V–Cr–SiO_2-(10)	160
20	V–Cr–γ-Al_2O_3-(20)	270	V–Cr–SiO_2-(20)	142

a) Cr/(V+Cr): 50 atom %. b) Cr/(V+Cr): 70 atom %. Both series were prepared from NH_4VO_3 and $Cr(NO_3)_3\cdot9H_2O$.

Table 2. Compositions of supported metal oxides, symbols, and specific surface areas of catalysts

Composition Cr/(V+Cr) (atom %)	G-series[a]		H-series[b]		I-series[c]	
	Symbol	S_s(m²/g)	Symbol	S_s(m²/g)	Symbol	S_s(m²/g)
0	G-0	261	H-0	255	I-0	109
20	G-2	274			I-2	105
30			H-3	268		
40	G-4	282			I-4	124
50	G-5	265	H-5	249		
60	G-6	260			I-6	132
70			H-7	232	I-7	138
80	G-8	252			I-8	131
100	G-10	244	H-10	212	I-10	136

a) Prepared from NH_4VO_3, $Cr(NO_3)_3 \cdot 9H_2O$, and alumina hydrate. b) Prepared from NH_4VO_3, $(NH_4)_2CrO_4$, and alumina hydrate. c) Prepared from NH_4VO_3, $Cr(NO_3)_3 \cdot 9H_2O$, and silica sol. The concentration of metal oxides (calculated as $V_2O_5+Cr_2O_3$) was 20 wt % in each series.

ethanol–solid carbon dioxide mixture to stop any further reaction, and the catalyst was allowed to settle. The clear liquid phase was then removed from the reactor for analysis.

Materials. The *t*-BuOOH was purified by vacuum distillation (40.0 °C/25 mmHg). The di-*t*-butyl peroxide (*t*-Bu_2O_2) obtained from the Nippon Kayaku Co. was shown to be pure by gas chromatography. The di-*t*-butyl ether (*t*-Bu_2O) was prepared by the method of West *et al.*[13] The other materials, *t*-butyl alcohol (*t*-BuOH), acetone, and 2-methyl propene were commercial products and were used without further purification. The benzene used as a solvent was purified by distillation.

Analytical Procedures. The decomposition products, *t*-BuOH, *t*-Bu_2O_2, acetone, 2-methyl propene, and *t*-Bu_2O, were identified by gas chromatography-mass spectrometry, using a Shimadzu LKB 9000 apparatus and using a 2-m column of PEG 6000 at an ionization voltage of 70 eV. The products were determined as follows. Part of the liquid sample was titrated for unconverted *t*-BuOOH by the iodometric method[12] using a mixture of 20 ml of 90:10 isopropyl alcohol–acetic acid and 1 g of NaI. *t*-Bu_2O_2 gave no titer in this method. The rest was treated with sufficient triphenylphosphine for the quantitative conversion of the *t*-BuOOH into *t*-BuOH,[14] and then analyzed for products by gas chromatography using a column of PEG 6000. The benzene used as a solvent was used as the internal standard. Part of the 2-methyl propene formed was detected in the gas phase and was determined by gas chromatography using a column of DMS.

The analytical results of the supported V–Cr catalysts obtained by means of X-ray diffraction, X-ray photoelectron spectroscopy (XPS), and infrared absorption were reported in the preceding paper.[1] The surface area has been determined by the BET method.[1] In the present work, we measured the electron-spin resonance (ESR) and the surface acidity of the catalyst. The ESR spectra of the catalyst evacuated at 400 °C for 2 h were recorded with a JEOL-JES-ME3X spectrometer at 25 °C and at −196 °C. The acid strength and acidity of the catalyst were measured by a butylamine titration method using 4-(phenylazo)-diphenylamine ($pK_a=1.5$) and Methyl Red ($pK_a=4.8$) as Hamett indicators. Silica–alumina, the acidity of which was 0.44 and 0.14 mmol/g in the ranges of $pK_a \leqq 1.5$ and $1.5 < pK_a \leqq 4.8$ respectively, was used as the internal standard because nearly all of the catalysts are strongly coloured.[15]

Results and Discussion

Decomposition of t-*BuOOH with the Me(acac)$_n$ Catalyst.*

Table 3. Rate constants and products distributions for the acetylacetonato-catalyzed decomposition of *t*-BuOOH[a]

Catalyst	k_1/s^{-1} [b]	*t*-BuOOH conversion (%)	Product selectivity				Reaction time (min)
			t-BuOH (%)[c]	*t*-Bu_2O_2 (%)[c]	Acetone (%)[c]	2-Methyl-propene (%)[c]	
$Co(acac)_2$	7.68×10^{-3}	98.6	81.0	12.3	3.3	—	120
$Mn(acac)_3$	1.92×10^{-4}	93.2	84.0	9.5	2.0	0.7	240
$Cr(acac)_3$[d]	1.59×10^{-4}	96.5	78.9	12.5	2.9	—	300
$Mn(acac)_2$	1.48×10^{-4}	90.1	79.8	13.7	4.1	0.5	240
$VO(acac)_2$	1.41×10^{-4}	85.0	81.1	10.5	3.2	3.0	300
$Co(acac)_3$	8.42×10^{-5}	72.0	82.1	11.3	4.0	—	300
$Cu(acac)_2$	1.07×10^{-5}	13.2	82.1	5.7	1.6	—	300
$MoO_2(acac)_2$	9.1×10^{-6}	7.4	72.9	8.3	4.5	5.3	300
$Ni(acac)_2$	4.5×10^{-6}	2.3	—	—	—	—	300
$TiO(acac)_2$	4.0×10^{-6}	2.5	—	—	—	—	300
$Fe(acac)_3$	3.7×10^{-6}	3.0	—	—	—	—	300

a) The concentrations of *t*-BuOOH and Me(acac)$_n$ were 10^{-1} and 10^{-5} mol/l respectively in benzene. The reaction temperature was 60 °C. b) First-order rate constants. c) Mol % based on *t*-BuO groups found. d) $Cr(acac)_3$ showed an induction period of about 30 min.

Table 3 shows the results of the decomposition of *t*-BuOOH with various metal acetylacetonate catalysts. In the absence of a catalyst, no reaction was observed. The decrease in the concentration of *t*-BuOOH obeyed good first-order kinetics in all reactions; accordingly, the activity of the metal ion is expressed by the first-order rate constant (k_1). Only $Cr(acac)_3$ showed an induction period (about 30 min), probably because of the stability of its chelate structure. Similar product distributions were observed for nearly all reactions; *i.e.*, the selectivities of the products were as follows: *t*-BuOH, 80%; $t\text{-Bu}_2O_2$, 10%, and acetone, 5%. When the reactions gave a sufficiently high conversion, *i.e.*, in the use of the chelates of Co, Mn, or Cr, the gas chromatography indicated the formation of a small amount of formaldehyde (not estimated quantitatively). The results can be interpreted by the following reaction scheme, which was been proposed in the literature:[4-12]

$$2t\text{-BuOOH} \xrightarrow{M^{n+}/M^{(n+1)+}} t\text{-BuOO}\cdot + t\text{-BuO}\cdot + H_2O \quad (1)$$

$$t\text{-BuO}\cdot + t\text{-BuOOH} \longrightarrow t\text{-BuOH} + t\text{-BuOO}\cdot \quad (2)$$

$$2t\text{-BuOO}\cdot \longrightarrow 2t\text{-BuO}\cdot + O_2 \quad (3)$$

$$2t\text{-BuOO}\cdot \longrightarrow t\text{-Bu}_2O_2 + O_2 \quad (4)$$

$$t\text{-BuO}\cdot \longrightarrow CH_3COCH_3 + CH_3\cdot \quad (5)$$

$$CH_3\cdot + O_2 \longrightarrow CH_3OO\cdot \quad (6)$$

$$CH_3OO\cdot + t\text{-BuOO}\cdot \longrightarrow CH_2O + t\text{-BuOH} + O_2 \quad (7)$$

The *t*-BuOOH is decomposed homolytically into peroxy and alkoxy radicals by the Haber-Weiss mechanism (1), followed by the induced decomposition (2) and the competitive reactions of peroxy radicals (3 and 4). Some of *t*-butoxyl radicals are separated into acetones and methyl radicals (5);[5,6,12] the latter products are then converted into formaldehyde (6 and 7).[10-12] Generally speaking, the choice of the metal ion, as long as it can undergo a facile one-electron redox reaction, seems to have little influence on the products. It is worth noting that the chelates of vanadium and chromium showed sufficiently high activities compared with cobalt and manganese chelates.

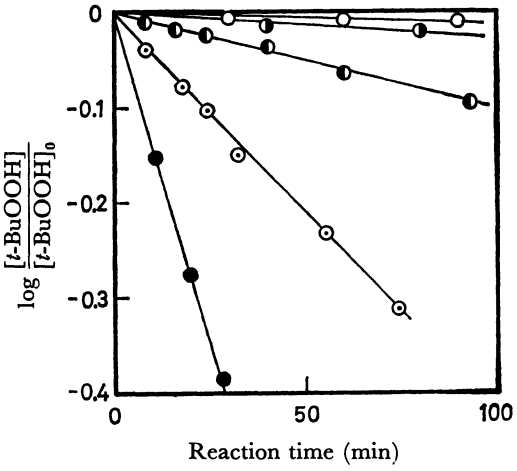

Fig. 1. Decomposition of *t*-BuOOH with V–Cr–γ-Al_2O_3.
The concentration of *t*-BuOOH and the catalyst were 10^{-1} mol/l and 5 g/l respectively in benzene. The raction temperature was 60°C. Cr/(V+Cr)=0.5.
○: γ-Al_2O_3, ◑: V–Cr–γ-Al_2O_3 (1), ◐: V–Cr–γ-Al_2O_3 (5), ⊙: V–Cr–γ-Al_2O_3 (10), ●: V–Cr–γ-Al_2O_3 (20).

Effect of the Amount of Metal Oxides Supported. As is shown in the results of the decomposition of *t*-BuOOH with the V–Cr–γ-Al_2O_3 catalyst (Fig. 1), good first-order rate plots were obtained up a conversion of 40% with the heterogeneous catalysts also. The first-order rate constants thus obtained are shown in Table 4, together with the product distribution when the amount of supported metal oxides varied. Both systems, *i.e.*, V–Cr–γ-Al_2O_3 and V–Cr–SiO_2, showed product distributions similar to that obtained with $Me(acac)_n$ catalysts, except that the V–Cr–SiO_2 system gave small amounts of 2-methyl propene and $t\text{-Bu}_2O$. Therefore, it may reasonably be considered that the decomposition of *t*-BuOOH on the present heterogeneous catalysts is initiated by the redox reaction 1 and that it then proceeds mainly by means of the radical chain reactions 2—7.

Table 4. Rate constants and product distributions for the V–Cr–γ-Al_2O_3 or –SiO_2-catalyzed decomposition of *t*-BuOOH[a]

Catalyst	k_1/s^{-1} [b]	*t*-BuOOH conversion (%)	Product selectivity[c]					Reaction time (min)
			t-BuOH (%)	$t\text{-Bu}_2O_2$ (%)	Acetone (%)	2-Methyl-propene (%)	$t\text{-Bu}_2O$ (%)	
γ-Al_2O_3	3.8×10^{-6}	1.5	—	—	—	—	—	300
V–Cr–γ-Al_2O_3(1)	8.8×10^{-6}	9.0	67.0	13.1	2.3	—	—	300
V–Cr–γ-Al_2O_3(5)	3.7×10^{-5}	64.7	85.4	9.0	3.0	—	—	300
V–Cr–γ-Al_2O_3(10)	1.65×10^{-4}	91.5	84.7	12.8	2.1	—	—	240
V–Cr–γ-Al_2O_3(20)	5.37×10^{-4}	96.1	82.3	14.9	2.1	—	—	180
SiO_2	1.3×10^{-5}	2.6	—	—	—	—	—	300
V–Cr–SiO_2(1)	3.99×10^{-3}	99.5	79.4	15.3	2.6	tr	—	180
V–Cr–SiO_2(5)	4.42×10^{-3}	99.8	84.9	9.8	4.1	0.1	tr	120
V–Cr–SiO_2(10)	4.65×10^{-3}	99.8	84.1	10.0	4.8	0.1	tr	120
V–Cr–SiO_2(20)	4.24×10^{-3}	98.9	82.9	11.6	4.4	0.2	tr	120

a) The concentrations of *t*-BuOH and the catalyst were 10^{-1} mol/l and 5 g/l respectively in benzene. The reaction temperature was 60 °C. b) First-order rate constants. c) Mol % based on *t*-BuO groups found.

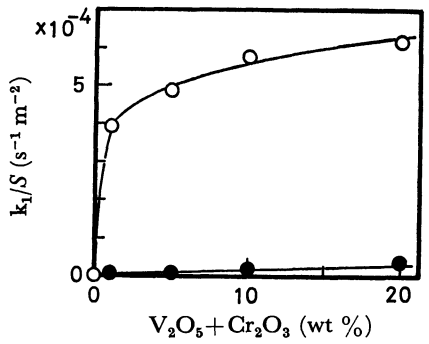

Fig. 2. Specific activity of V–Cr–γ-Al_2O_3 or –SiO_2 series catalyst for the decomposition of *t*-BuOOH.
●: V–Cr–γ-Al_2O_3 (Cr/(V+Cr)=0.5), ○: V–Cr–SiO_2 (Cr/(V+Cr)=0.7).

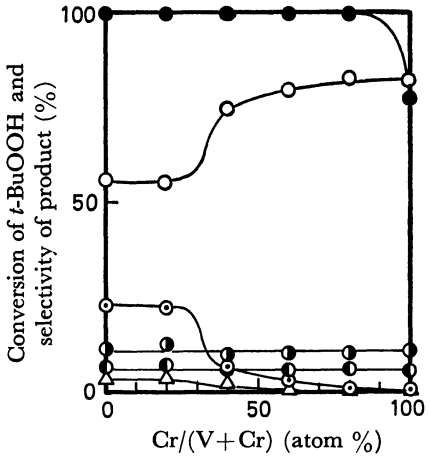

Fig. 3. Product distribution in the 4 h decomposition of *t*-BuOOH with I-series catalysts.
The concentration of *t*-BuOOH and the catalyst were 10^{-1} mol/l and 5 g/l respectively in benzene. The reaction temperature was 60 °C.
●: Conversion of *t*-BuOOH, Selectivity; ○: *t*-BuOH, ◑: t-Bu_2O_2, ◐: acetone, ⊙: 2-methyl propene, △: t-Bu_2O.

The decomposition proceeds rapidly on the V–Cr–SiO_2 system; this is more clearly observed in Fig. 2, which shows the specific activity of each system. It is noteworthy that the activity increased rapidly when a small amount of metal oxides was supported on SiO_2; on the contrary, no such rapid increase was observed on γ-Al_2O_3. A similar tendency of the activity was also observed when the binary catalysts were used in the oxidation of cyclohexene (see Fig. 4 in the preceding paper[1]).

Effects of Composition and Raw Materials of Metal Oxides. The systems supported on γ-Al_2O_3, *i.e.*, G- and H-series, gave product distributions similar to those obtained with a soluble Co or Mn chelate catalyst, while a different distribution was observed with the I-series, especially those with a high vanadium content, on SiO_2 (Table 5). That is, the I-series gave 2-methyl propene and t-Bu_2O, too, and the higher vanadium content increased the selectivity of the two products while decreasing that of *t*-BuOH. Such a tendency was observed more clearly after decomposition for 4 h (Fig. 3); the selectivities of 2-methyl propene and t-Bu_2O increased at the expense of that of *t*-BuOH when the I-0, I-2, and I-4 catalysts were used. The selectivity of t-Bu_2O_2 or acetone did not change over all the compositions of the I-series catalysts. The I-series

TABLE 5. RATE CONSTANTS AND PRODUCT DISTRIBUTIONS FOR THE G-, H-, OR I- SERIES CATALYZED DECOMPOSITION OF *t*-BuOOH[a]

Catalyst	k_1/s^{-1} [b]	*t*-BuOOH conversion (%)	Product selectivity[c]					Reaction time (min)
			t-BuOH (%)	t-Bu_2O_2 (%)	Acetone (%)	2-Methyl-propene (%)	t-Bu_2O (%)	
G-0	2.07×10^{-4}	90.2	83.9	10.5	4.8	0.2	—	240
G-2	2.79×10^{-4}	89.7	84.1	13.0	2.3	0.1	—	180
G-4	4.27×10^{-4}	93.1	84.1	12.1	2.8	0.2	—	180
G-5	5.37×10^{-4}	96.1	82.3	14.9	2.1	—	—	180
G-6	4.96×10^{-4}	96.3	81.3	14.0	2.8	—	—	180
G-8	4.13×10^{-4}	90.0	85.9	10.0	3.2	—	—	180
G-10	9.5×10^{-6}	17.8	70.3	12.5	5.0	—	—	240
H-0	1.91×10^{-4}	87.3	85.3	12.1	3.2	0.2	—	240
H-3	3.67×10^{-4}	84.4	83.6	10.7	4.4	—	—	180
H-5	5.35×10^{-4}	94.2	82.4	11.8	4.7	—	—	180
H-7	5.59×10^{-4}	97.1	83.8	10.6	5.1	—	—	180
H-10	7.42×10^{-4}	98.6	83.6	10.0	5.0	—	—	180
I-0	5.64×10^{-3}	99.2	75.6	10.5	5.8	7.2	0.6	120
I-2	5.28×10^{-3}	99.0	75.8	10.9	5.9	6.5	0.8	120
I-4	4.56×10^{-3}	98.5	79.7	11.9	5.8	1.3	0.3	120
I-6	4.16×10^{-3}	97.6	82.0	11.8	5.3	0.5	tr	120
I-8	3.41×10^{-3}	98.2	82.7	11.0	4.4	0.2	tr	120
I-10	1.26×10^{-3}	78.6	83.0	11.8	4.9	0.2	tr	240

a) The concentrations of *t*-BuOOH and the catalyst were 10^{-1} mol/l and 5 g/l respectively in benzene. The reaction temperature was 60 °C. b) First-order rate constants. c) Mol % based upon *t*-BuO groups found.

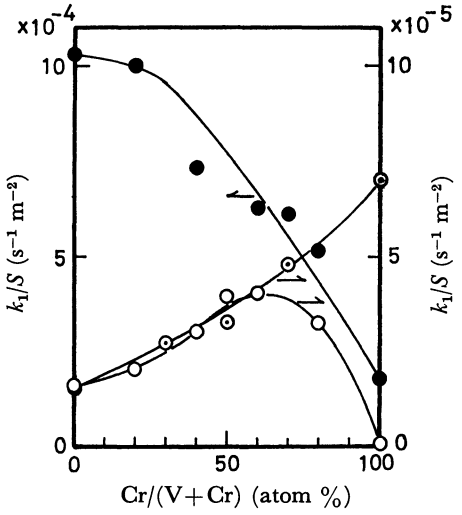

Fig. 4. Specific activity of G-, H-, and I-series catalyst for the decomposition of *t*-BuOOH.
The concentration of *t*-BuOOH and the catalyst were 10^{-1} mol/l and 5 g/l respectively in benzene. The reaction temperature was 60 °C.
○: G-series, ⊙: H-series, ●: I-series.

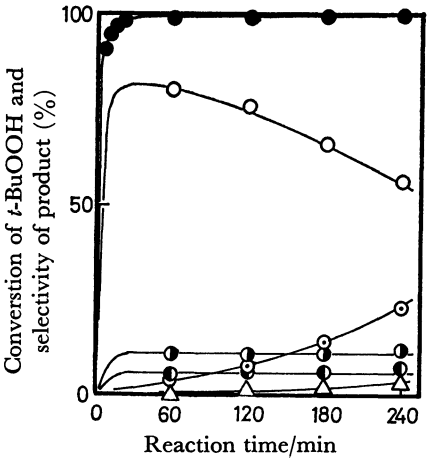

Fig. 5. Decomposition of *t*-BuOOH with I-0 catalyst.
The concentration of *t*-BuOOH and the catalyst were 10^{-1} mol/l and 5 g/l respectively in benzene. The reaction temperature was 60 °C.
●: Conversion of *t*-BuOOH. Selectivity; ○: *t*-BuOH, ◑: t-Bu_2O_2, ◐: acetone ⊙: 2-methyl propene, △: t-Bu_2O.

catalysts gave higher decomposition rates than the G- or H-series catalysts. The specific activities are shown in Fig. 4 in terms of k_1/S. When supported on SiO_2, a higher vanadium content resulted in a higher specific activity. Concerning the systems supported on γ-Al_2O_3, the use of $(NH_4)_2CrO_4$ (Cr^{6+}), *i.e.*, the H-series, instead of $Cr(NO_3)_3 \cdot 9H_2O$ (Cr^{3+}), *i.e.*, the G-series, as the raw material caused a markedly high activity at a high chromium content, while both series with low chromium contents showed similar activities. The fact that the H-series contains a higher valence state of chromium ions than the G-series has already been noted.[1] The binary system in the G-series clearly showed an increase in the activity, an increase which may be attributed to the formation of chromium isopolyvanadates, as has already been reported,[3] though the effect of the binary-system formation was not obvious in the I- and H-series.

The order of the activity mentioned above is well correlated with that observed in the oxidation of cyclohexene with the same catalyst systems[1] when the initial rate, R_{max}-A, is adopted as the activity of the I-series (Fig. 5 in the preceding paper[1]). That is, though the O_2 absorption rate shown by I-0 or I-2 in the steady state of cyclohexene oxidation, R_{max}-B, was much lower than would be expected from the *t*-BuOOH decomposition, the initial rate, R_{max}-A, was sufficiently high, in agreement with the decomposition rate. Thus, it may reasonably be considered that the main role of the binary catalyst in the oxidation of cyclohexene is in the acceleration of the homolysis of hydroperoxide.

Dehydration of t-*BuOH on the* V_2O_5–SiO_2 *Catalyst.* Tables 4 and 5 and Fig. 3 reveal that 2-methyl propene and t-Bu_2O were formed, together with the radical-reaction products, when the SiO_2-supported catalysts with a higher vanadium content were used. The amounts of 2-methyl propene and t-Bu_2O increased at the expense of *t*-BuOH; the amount of 2-methyl propene was, further, about 10 times that of t-Bu_2O. In order to clarify the mechanism of the formation of the two products, the variation in their selectivities during the reaction was examined by using the I-0 catalyst (Fig. 5). The decomposition of *t*-BuOOH was finished within about 30 min after the beginning of the reaction. The selectivity of *t*-BuOH reached its maximum value and then decreased gradually during 4 h of reaction; 2-methyl propene and t-Bu_2O took the place of *t*-BuOH. In contrast, no change was observed in the selectivities of t-Bu_2O_2 and acetone. The I-2 catalyst also showed a similar behavior. Thus, the dehydration of *t*-BuOH is suggested on the I-0 or I-2 catalyst. For the purpose of confirming this possibility, a solution of *t*-BuOH in benzene was treated at 60 °C with the I-2 catalyst in an N_2 atmosphere (Fig. 6). The dehydration of *t*-BuOH into 2-methyl propene was clearly observed, though t-Bu_2O was not detected; a similar phenomenon was also observed with

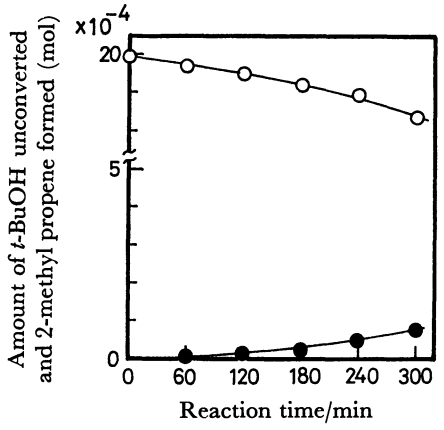

Fig. 6. Dehydration of *t*-BuOH with I-2 catalyst.
The concentration of *t*-BuOOH and the catalyst were 2×10^{-1} mol/l and 5 g/l respectively in benzene. The reaction was carried out under N_2 atmosphere at 60 °C.
○: *t*-BuOH, ●: 2-methyl propene.

the I-0 catalyst. It can, therefore, be concluded that the following dehydrations were catalyzed on the SiO_2-supported system with a high vanadium content:

$$t\text{-BuOH} \longrightarrow CH_3\text{-}C(CH_3)=CH_2 + H_2O \quad (8)$$

$$2t\text{-BuOH} \longrightarrow t\text{-}Bu_2O + H_2O \quad (9)$$

The probability of the intramolecular dehydration (8) may reasonably be larger than that of the intermolecular one (9), resulting in the higher selectivity of 2-methyl propene (Fig. 5). I-0 showed the X-ray diffraction lines of V_2O_5 crystals; I-2, on the contrary, showed no line,[1] and both the systems catalyzed the dehydration. Therefore, the active species for the dehydration on the catalysts seems to be composed of the vanadium oxide–SiO_2 system.

Co-ordination State of a Metal on a Catalyst. The analytical results of X-ray diffraction, infrared absorption, and XPS have been reported in the preceding paper.[1] The XPS analysis revealed that several valence states of chromium, *i.e.*, Cr^{6+}, Cr^{5+}, and Cr^{3+}, exist on the supported catalysts. On γ-Al_2O_3, the H-series prepared from $(NH_4)_3CrO_4$(Cr^{6+}) includes chromium ions of a higher valence state than the G-series from $Cr(NO_3)_3 \cdot 9H_2O$ (Cr^{3+}) at a high chromium content, though the valence state of vanadium was not clearly assigned. Such valence states of metal contributed considerably to the activity for the cyclohexene oxidation[1] and also for the *t*-BuOOH decomposition (Fig. 4); the configuration of metal complexes on the catalyst surface seemed, however, to play a more important role.[1] In order to obtain information about the metal-complex configurations, the ESR spectra were measured.

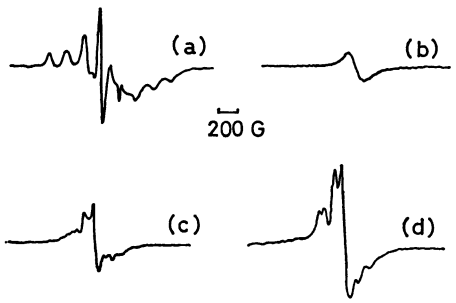

Fig. 7. ESR spectra of the supported vanadia systems.
(a) G-0 at 25 °C, (b) I-0 at 25 °C, (c) I-0 at 25 °C after an exposure to atmosphere at room temperature, (d) I-0 at −196 °C.

The spectra of the supported vanadia systems are shown in Fig. 7. At 25 °C, V_2O_5–γ-Al_2O_3 (G-0) exhibited a characteristic spectrum (a) with hfs due to ^{51}V(IV) in the octahedral (or distorted square pyramidal) co-ordination (VO_5),[16-21] whereas V_2O_5–SiO_2 (I-0) gave a very weak singlet spectrum (b), the line shape of which was nearly Lorentzian. At room temperature, the tetrahedrally co-ordinated V(IV) ions (VO_4) could not be detected by ESR.[16,20,22] Moreover, I-0 showed a clear X-ray diffraction pattern of the V_2O_5 crystal.[1] The (b) spectrum may, therefore, be assigned to V(IV) ions attributable to lattice defects in the V_2O_5 crystal. I-0 showed a spectrum (d) at the temperature of −196 °C; its line shape differed from (a) and (b), probably indicating the (VO_4) formation, as was suggested in the preceding paper.[1] Suzuki *et al.*[20] and Van Reijen *et al.*[16] also detected tetrahedrally co-ordinated V(IV) ions on the V_2O_5–SiO_2 system by ESR at low temperatures. The (b) spectrum became slightly strong and simultaneously anisotropic (c) when the evacuated I-0 was exposed to atmosphere at room temperature. Van Reijen reported that (VO_4) is very sensitive to atmosphere; for example, after the admission of water vapor at room temperature, (VO_4) changes probably to (VO_5), which is sufficiently stable and is detected at room temperature.[16] The (c) spectrum may be of V(IV) ions both in the V_2O_5 lattice defects and in (VO_5). Thus, two types of configurations of vanadium complexes, *i.e.*, (VO_5) on γ-Al_2O_3 and (VO_4) on SiO_2, are recognized.

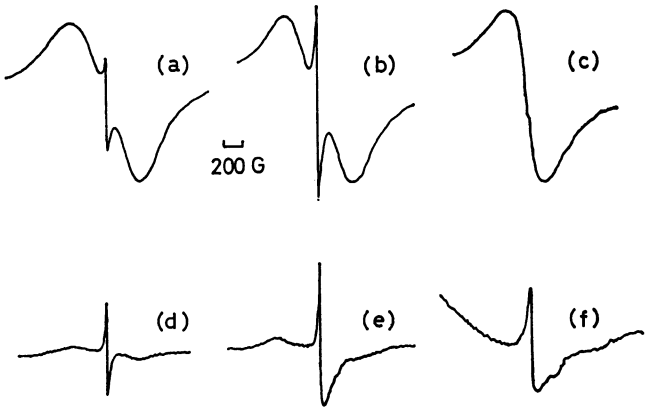

Fig. 8. ESR spectra of the supported chromia systems.
(a): G-10 at 25 °C, (b): H-10 at 25°C, (c): I-10 at 25 °C, (d): G-10 at −196 °C, (e): H-10 at −196 °C, (f): I-10 at −196 °C.

Figure 8 shows the spectra of the supported chromia systems. According to the analytical results obtained by the use of XPS,[1] these systems contained Cr^{5+} and Cr^{3+} ions which can be detected by ESR. X-Ray diffraction measurements showed that the Cr_2O_3 crystal grew on SiO_2, but not on γ-Al_2O_3.[1] Therefore, we can presume that, on γ-Al_2O_3, most of the Cr^{3+} is present in solution in the γ-Al_2O_3 lattice; on SiO_2, though, it is present mainly in a separate chromia phase. At room temperature, the ESR spectra of the Cr_2O_3–γ-Al_2O_3 systems (G-10 and H-10) showed a very broad band and another, relatively sharp peak, characterized by a *g*-factor of 1.97 and a linewidth of approximately 50 G, superimposed on it (a and b). The ratio of the intensities of the two bands varied considerably. The narrow signal may be assigned to the Cr^{5+} ions (the so-called γ-phase), whereas the broad one may be assigned to the Cr^{3+} ions (the β-phase).[24,25] The intensity of the γ-phase was as follows: H-10>G-10; the Cr^{5+} ions are more abundant on the Cr_2O_3–γ-Al_2O_3 system prepared from $(NH_4)_2CrO_4$ than on that prepared from $Cr(NO_3)_3 \cdot 9H_2O$. This was in good agreement with the result obtained by the XPS measure-

ment.[1] The Cr_2O_3–SiO_2 (I-10) showed a spectrum similar to those of the Cr_2O_3–γ-Al_2O_3, though the intensity of the narrow band was very weak (c). The broad band may be assigned to the separate phase of the Cr_2O_3 crystals, which was detected by the X-ray analysis.[1] When the sample was cooled to −196 °C. The form of the spectrum changed appreciably; the intensity of the broad band was weakened. Moreover, the narrow signal of I-0 became stronger, accompanied by a marked anisotropy of its *g*-factor (f). The anisotropic signal may be assigned to the Cr^{5+} ions tetrahedrally co-ordinated (CrO_4), which are characterized by a small spin-lattice relaxation time and which are, accordingly, observed only at low temperatures.[16,23] The anisotropy was also observed in the narrow signal of the H-10 catalyst (e). However, G-10 gave a strong, narrow signal of the Cr^{5+} ions co-ordinated octahedrally (d).[23,26] These results can be summarized as follows: the Cr^{5+} ions are mainly co-ordinated tetrahedrally (CrO_4) on SiO_2 and octahedrally (or square-pyramidally) (CrO_5) on γ-Al_2O_3. In the latter case, however, the tetrahedral co-ordination may also occur on the H-series with a high chromium content, because the anisotropy was observed with H-10 at −196 °C, as has been mentioned above. This is supported by the fact that the tetrahedral $(CrO_4)^{3-}$ ions are preferentially found in a highly alkaline solution;[27] an H-series with a high chromium content was prepared from $(NH_4)_2CrO_4$, *i.e.*, in alkaline media. It may also be reasonable to assume that the (CrO_4) tetrahedron is linked to the SiO_2 network by sharing corners or edges with the SiO_4 tetrahedron, because the SiO_2 crystal has a tetrahedral structure.[16,23]

Acidity of Catalyst. The acidities of the supported catalysts obtained by means of the butylamine titration method are shown in Fig. 9; they are classified into two kinds of acid strengths, *i.e.*, $pK_a \leqq 1.5$ and $1.5 < pK_a \leqq 4.8$. γ-Al_2O_3 itself showed a strong acidity, whereas a weak acidity alone was observed on SiO_2. It is noteworthy that, when a small amount of V–Cr binary oxide was added to SiO_2, a remarkable increase in the strong acid sites was observed. On γ-Al_2O_3, the acidity

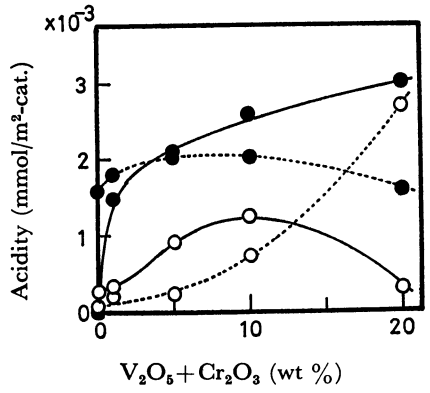

Fig. 9. Acidity on V–Cr–γ-Al_2O_3 or –SiO_2 system catalyst.
●: $pK_a \leqq 1.5$, ○: $1.5 < pK_a \leqq 4.8$.
——: V–Cr–SiO_2, (Cr/(V+Cr)=0.7), ------: V–Cr–γ-Al_2O_3, (Cr/(V+Cr)=0.5).

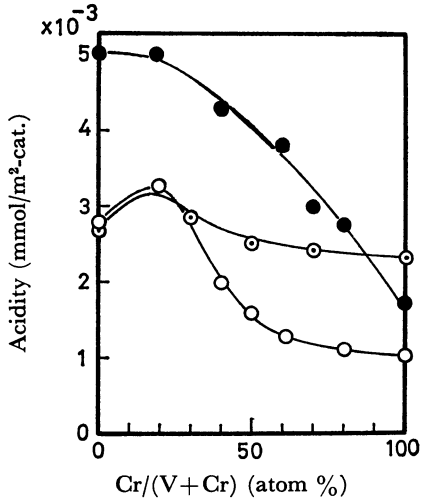

Fig. 10. Acidity of $pK_a \leqq 1.5$ on G-, H-, and I-series catalysts.
○: G-series, ⊙: H-series, ●: I-series.

of $pK_a \leqq 1.5$ did not vary upon the addition of the binary oxide; that of $1.5 < pK_a \leqq 4.8$, however, enhanced by its addition in sufficient amount. The strong acidities ($pK_a \leqq 1.5$) of the three series of catalysts, *i.e.*, the I-, H-, and G-series, are shown in Fig. 10 as the function of the chromium content. The largest acidity was given on SiO_2, whereas, on γ-Al_2O_3, the system prepared from $(NH_4)_2CrO_4$ showed a larger acidity than that prepared from $Cr(NO_3)_3 \cdot 9H_2O$, especially at high chromium contents. When the activities in Figs. 2 and 4 are compared to the acidities in Figs. 9 and 10 respectively, it seems that the activity for the decomposition of *t*-BuOOH is related to the acidity on the supported catalyst. A clear-cut correlation was observed particularly with the V–Cr–SiO_2 series (Fig. 2) and the I-series (Fig. 4), which are both supported on SiO_2. Both the activity and the acidity were at a maximum on the V_2O_5–SiO_2 system (I-0), in which the tetrahedral configuration was detected by ESR. The strength of the acidity of (VO_4) may be sufficiently large to dehydrate *t*-BuOH, as has been described already. The acidity observed on the Cr_2O_3–SiO_2 catalyst may be related to the tetrahedral (CrO_4) configuration, which is formed newly, because SiO_2 showed no acidity ($pK_a \leqq 1.5$) itself.

When supported on γ-Al_2O_3, which itself showed acidity, the correlation was not so clear as on SiO_2, but at a high chromium content the catalyst of the H-series, on which the (CrO_4) configuration was observed, showed both a higher activity and a higher acidity compared to the G-series catalysts. Thus, this higher acidity seems also to be related to the tetrahedral (CrO_4) configuration.

Though the details of the mechanism by which the acidic sites contribute to the autoxidation are not yet clear, it may be suggested that the tetrahedral complexes work both as acidic sites and as active sites for the homolytic decomposition of hydroperoxide, through which process the autoxidation is accelerated. The homolytic decomposition may proceed *via* the co-ordination of hydroperoxide to a vacant site in the

complex; the vacant site is also suspected to behave as an acidic site.

In conclusion, the activity for the cyclohexene oxidation (Fig. 5 in the preceding paper[1]) correlates fairly well with that for the *t*-BuOOH decomposition, supporting the theory of the oxidation mechanism which proceeds *via* the radical decomposition of hydroperoxide. The effects of the V–Cr binary-system formation was not so clear in the *t*-BuOOH decomposition as in the cyclohexene oxidation, but the interaction between the metal oxides and the supports strongly affected the activity for the *t*-BuOOH decomposition. The oxidation activity of the I-series (Fig. 5 in the preceding paper[1]), when compared with those of other series, was considerably lower than would be expected from the *t*-BuOOH decomposition (Fig. 4); such a lowering was most clearly observed at a high vanadium content. This may be due to the instability of the (VO_4) structure: this effect was not clearly observed in the *t*-BuOOH decomposition, which proceeded rapidly, but was recognized in a relatively slow reaction such as the cyclohexene oxidation.

References

1) K. Takehira, T. Hayakawa, and T. Ishikawa, *Bull. Chem. Soc. Jpn.*, **52**, 697 (1979).
2) K. Takehira and T. Ishikawa, *Bull. Chem. Soc. Jpn.*, **49**, 2351 (1976).
3) K. Takehira, T. Hayakawa, and T. Ishikawa, *Bull. Chem. Soc. Jpn.*, **51**, 1685 (1978).
4) R. Hiatt, K. C. Irwin, and C. W. Gould, *J. Org. Chem.*, **33**, 1430 (1968).
5) R. Hiatt, T. Mill, and F. R. Mayo, *J. Org. Chem.*, **33**, 1416 (1968).
6) W. H. Richardson, *J. Am. Chem. Soc.*, **87**, 247 (1965).
7) W. H. Richardson, *J. Am. Chem. Soc.*, **87**, 1096 (1965).
8) P. D. Bartlett and T. G. Traylor, *J. Am. Chem. Soc.*, **85**, 2407 (1963).
9) C. Walling and A. Padwa, *J. Am. Chem. Soc.*, **85**, 1593 (1963).
10) M. H. Dean and G. Skirrow, *Trans. Faraday Soc.*, **54**, 849 (1958).
11) F. H. Seubold, F. F. Rust, and W. E. Vaughan, *J. Am. Chem. Soc.*, **73**, 18 (1951).
12) R. Hiatt, T. Mill, K. C. Irwin, and J. K. Castleman, *J. Org. Chem.*, **33**, 1421 (1968).
13) R. West, D. L. Powell, M. K. T. Lee, and L. S. Whatley, *J. Am. Chem. Soc.*, **86**, 3228 (1968).
14) L. Horner and W. Jurgleit, *Ann. Chem.*, **591**, 139 (1955).
15) T. Sukeno and T. Shirasaki, *Nippon Kagaku Kaishi*, **1973**, 2229.
16) L. L. Van Reijen and P. Cossee, *Discuss. Faraday Soc.*, **41**, 277 (1966).
17) H. Takahashi, M. Shiotani, H. Kobayashi, and J. Sohma, *J. Catal.*, **14**, 134 (1969).
18) M. Akimoto, M. Usami, and E. Echigoya, *Bull. Chem. Soc. Jpn.*, **51**, 2195 (1978).
19) S. Yoshida, T. Iguchi, S. Ishida, and K. Tarama, *Bull. Chem. Soc. Jpn.*, **45**, 376 (1972).
20) T. Suzuki, S. Yoshida, and K. Tarama, presented at the 37th National Meeting of the Chemical Society of Japan, Tokyo, April 1978.
21) C. J. Ballhausen and H. B. Gray, *Inorg. Chem.*, **1**, 111 (1962).
22) L. L. Van Reijen, P. Cossee, and H. J. Van Haren, *J. Chem. Phys.*, **38**, 572 (1963).
23) V. B. Kazanskii, *Kinet. Katal.*, **11**, 455 (1970).
24) C. P. Poole, Jr., W. L. Kehl, and D. S. MacIber, *J. Catal.*, **1**, 407 (1962).
25) D. E. O'Reilly and D. S. MacIber, *J. Phys. Chem.*, **66**, 276 (1962).
26) V. V. Voevodskii, *Proc. Int. Congr. Catal., 3rd* 1964, **1**, 88 (1965).
27) N. Bailey and M. C. R. Symos, *J. Chem. Soc.*, **1957**, 203.